der specific pathogen-free conditions. Seven to nine young (10–11 weeks) or aged (56–60 weeks) mice, for each strain, were used in each experiment. Mice were sacrificed, and their livers and pancreata were immediately removed, frozen on dry ice, and stored at −80 °C for biochemical studies.

8-Hydroxy-2′-deoxyguanosine (8-OHdG) was used as oxidative DNA damage marker and was detected as described previously [11]. DNA was extracted by incubating tissue homogenates with proteinase K (50 units/ml, Applied Biosystems, Foster City, CA) at 60 °C for 2 h, precipitated with ethanol and then dissolved in distilled water. After being incubated with nuclease P1 (60 units/ml, Seikagaku Corporation, Tokyo, Japan) and alkaline phosphatase (6 units/ml, Sigma Chemical Co, St. Louis, MO, USA) sequentially, 8-OHdG and dG contents were then detected by HPLC with electrochemical and UV detectors (Coulochem II, ESA, Chelmsford, MA), respectively. Data are expressed as the molar ratio of 8-OHdG to 10^5 dG.

Protein carbonyl contents reflecting oxidative protein damage were detected as previously described [12]. Proteins were extracted from tissues in the presence of proteinase inhibitor cocktails (0.5 μg/ml aprotinin, 0.7 μg/ml pepstatin, 0.5 μg/ml leupeptin; Sigma) in phosphate buffer (pH 7.5). Samples were incubated on ice for 15 min, and centrifuged at 10,000 × *g* for 15 min. The supernatants containing 2–3 mg proteins were incubated with four volumes of 10 mM 2,4-dinitrophenylhydrazine (DNPH, Nacalai Tesque, Kyoto, Japan) in 2 M HCl at room temperature for 1 h in the dark. This resulted in the formation of 2,4-dinitrophenyl adducts on proteins by reacting protein carbonyl with DNPH. Proteins were precipitated with an equal volume of 20% and 10% TCA sequentially, washed with ethanol:ethyl acetate (1:1), and resuspended in 6 M guanidine hydrochloride (Nacalai Tesque) in 20 mM phosphate buffer/trifluoroacetic acid (pH 2.3) for spectrophotometric analysis. Carbonyl contents were calculated using a molar extinction coefficient of 22.0 mM^{-1} cm^{-1} and expressed as nmol carbonyl/mg protein.

In order to know how age and inflammation affect oxidative DNA damage, we compared 8-OHdG levels in the livers and pancreata of age-matched *aly/aly* and WT mice. As shown in Fig. 1, young *aly/aly* and WT mice had almost identical hepatic 8-OHdG levels. In *aly/aly* mice, there was a four-fold increase in liver 8-OHdG with aging (Fig. 1A; $P < 0.01$), while hepatic 8-OHdG levels of WT mice only increased 1.5-fold with aging (Fig. 1A; $P = 0.11$). Moreover, hepatic 8-OHdG levels of aged *aly/aly* mice were significantly higher than those of age-matched WT mice ($P < 0.01$). In pancreas, mean 8-OHdG levels in aged mice were approximately twice that in young mice for each genotype (Fig. 1B; $P < 0.05$ for WT mice, $P = 0.14$ for *aly/aly* mice). Although pancreatic 8-OHdG levels in aged *aly/aly* mice were higher than those of age-matched WT mice, the differences were not significant ($P = 0.29$).

Further, we examined how age and inflammation influence protein oxidative damage in livers and pancreata using protein carbonyl contents as a marker. As seen in Fig. 2,

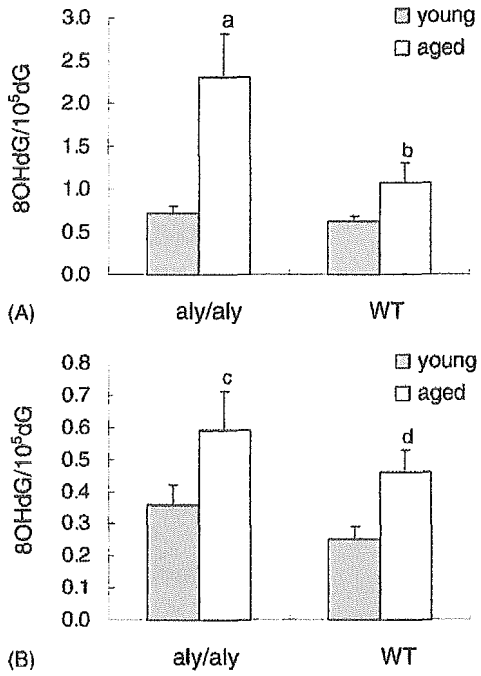

Fig. 1. Contents of 8-OHdG in DNA from the livers (A) and pancreata (B) of C57BL/6 *aly/aly* and WT mice. Aged mice: 56–60 weeks; young mice: 10–11 weeks. Data were obtained from seven to nine mice for each group and are represented as mean and standard error. Two-way analysis of variance was used to test for difference between groups. [a] $P < 0.05$ compared with both young *aly/aly* and aged WT mouse liver, [b] $P = 0.1148$ compared with young WT mouse liver, [c] $P = 0.1422$ compared with young *aly/aly* mouse pancreas, [d] $P < 0.05$ compared with young WT mouse pancreas.

hepatic carbonyl concentrations in aged *aly/aly* mice were virtually identical to those of aged WT mice (Fig. 2A). We did not find significant differences in hepatic carbonyl contents in young versus aged *aly/aly* mice, young versus aged WT mice, or young *aly/aly* versus young WT mice. In contrast to liver, carbonyl contents in the pancreata of aged WT mice were significantly higher than in pancreata of young WT mice (Fig. 2B, $P < 0.05$). However, pancreatic carbonyl concentrations in aged *aly/aly* mice were similar to those in young *aly/aly* mice. Unlike oxidative DNA damage in the livers, we did not observe significant differences in carbonyl levels in pancreas between aged *aly/aly* and WT mice.

This study showed a trend for age-dependent increases in oxidative damage to DNA in the liver and pancreas as measured by 8-OHdG level. Our results are in agreement with previous reports describing age-dependent increases in oxidative damage to DNA in multiple tissues including liver, kidney, brain, heart, intestine and pancreas [13,14]. Furthermore, we showed that oxidative damage to pancreatic proteins increased with increasing age only in WT whereas it was not seen in the livers of WT or *aly/aly* mice. In addition, analyzing oxidative lipid damage in the liver and pancreas using lipid peroxidation as a marker, we found that age did not cause lipid oxidative damage at our experimental settings (data not shown). These results support previous results that oxidative lipid and protein damages varied depending on

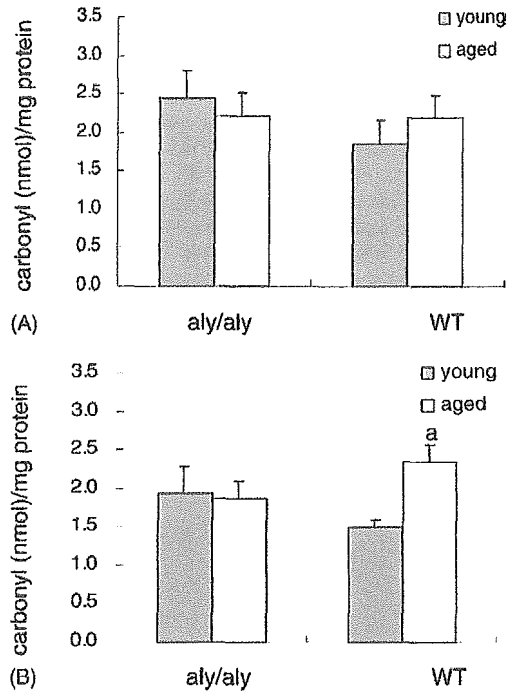

Fig. 2. Protein carbonyl contents in livers (A) and pancreata (B) of C57BL/6 *aly/aly* and WT mice. Data were obtained from seven to nine mice for each group and are represented as mean and standard error. Two-way analysis of variance was used to test for difference between groups. [a] $P < 0.05$ compared with young WT mice.

which tissues, cellular fractions and/or markers are examined [15–17].

More importantly, we found that 8-OHdG was highly accumulated only in inflamed livers of aged *aly/aly* mice but not in normal livers of aged WT mice. There was no significant correlation in 8-OHdG levels between liver and pancreas of *aly/aly* mice ($r = 0.25$, $P > 0.05$). These findings suggest that elevated 8-OHdG levels in inflamed livers of aged *aly/aly* mice are ascribed to liver inflammation but not to individual mouse variation. Previous studies have shown that oxidative DNA damage was usually accompanied by the damage to proteins and/or lipids in human inflamed liver diseases. For example, oxidative damages to DNA, lipids and proteins were seen in alcoholic liver disease [18]. Oxidative DNA damage coexisted with severe lipid damage in chronic hepatitis C more than in hepatitis B [19,20]. In our study, we did not find significant oxidative lipid and protein damages in the inflamed liver of aged *aly/aly* mice by measuring protein carbonyl contents and lipid peroxidation; our findings thus suggest that oxidative damage to DNA is more predominant than lipid and protein damages in inflamed livers of *aly/aly* mice.

High levels of ROS caused by their overproduction and/or failure to be removed by antioxidant enzymes lead to oxidative DNA damage. It has been shown that increasing age did not reduce antioxidant enzymes in mouse livers [13]. Inflammatory cells in the livers of aged *aly/aly* mice are mainly $CD4^+$ T cells [10]. Since T cells produce hydrogen peroxide and superoxide upon activation [4,21], ROS over-generated by infiltrated T cells may thus contribute to elevated 8-OHdG in the inflamed livers of aged *aly/aly* mice.

In summary, the present study showed that chronic inflammation in the livers, but not pancreata, of *aly/aly* mice led to elevated oxidative DNA damage without significant affects on lipids and proteins. It is thus possible that liver inflammation in aged *aly/aly* mice may be predisposed to tumorigenesis by enhancing 8-OHdG accumulation.

Acknowledgements

We thank Prof. Kanehisa Morimoto, Osaka University for his encouragement and Miss Chiko Yumiba, Kagoshima University for her administrative and technical assistance during this work. This work was supported by grants from the Japan Society for Science Promotion to BH Xu: C2-15590515 and T. Takeuchi: C2-12671664, and a Digestive Disease Center grant (DK56339) from the NIH.

References

[1] Cooke MS, Evans MD, Dizdaroglu M, Lunec J. Oxidative DNA damage: mechanisms, mutation, and disease. FASEB J 2003;17:1195–214.
[2] Floyd RA. Role of oxygen free radicals in carcinogenesis and brain ischemia. FASEB J 1990;4:2587–97.
[3] Bowler RP, Crapo JD. Oxidative stress in allergic respiratory diseases. J Allergy Clin Immunol 2002;110:349–56.
[4] MacMicking JD, Willenborg DO, Weidemann MJ, Rockett KA, Cowden WB. Elevated secretion of reactive nitrogen and oxygen intermediates by inflammatory leukocytes in hyperacute experimental autoimmune encephalomyelitis: enhancement by the soluble products of encephalitogenic T cells. J Exp Med 1992;176:303–7.
[5] Simmonds NJ, Allen RE, Stevens TR, Van Someren RN, Blake DR, Rampton DS. Chemiluminescence assay of mucosal reactive oxygen metabolites in inflammatory bowel disease. Gastroenterology 1992;103:186–96.
[6] Shimoda R, Nagashima M, Sakamoto M, Yamaguchi N, Hirohashi S, Yokota J, Kasai H. Increased formation of oxidative DNA damage, 8-hydroxydeoxyguanosine, in human livers with chronic hepatitis. Cancer Res 1994;54:3171–2.
[7] Dandona P, Thusu K, Cook S, Snyder B, Makowski J, Armstrong D, Nicotera T. Oxidative damage to DNA in diabetes mellitus. Lancet 1996;347:444–5.
[8] Bashir S, Harris G, Denman MA, Blake DR, Winyard PG. Oxidative DNA damage and cellular sensitivity to oxidative stress in human autoimmune diseases. Ann Rheum Dis 1993;52:659–66.
[9] Shinkura R, Kitada K, Matsuda F, Tashiro K, Ikuta K, Suzuki M, Kogishi K, Serikawa T, Honjo T. Alymphoplasia is caused by a point mutation in the mouse gene encoding Nf-kappa b-inducing kinase. Nat Genet 1999;22:74–7.
[10] Tsubata R, Tsubata T, Hiai H, Shinkura R, Matsumura R, Sumida T, Miyawaki S, Ishida H, Kumagai S, Nakao K, Honjo T. Autoimmune disease of exocrine organs in immunodeficient alymphoplasia mice: a spontaneous model for Sjogren's syndrome. Eur J Immunol 1996;26:2742–8.
[11] Nakajima M, Takeuchi T, Morimoto K. Determination of 8-hydroxydeoxyguanosine in human cells under oxygen-free conditions. Carcinogenesis 1996;17:787–91.

[12] Reznick AZ, Packer L. Oxidative damage to proteins: spectrophotometric method for carbonyl assay. Methods Enzymol 1994;233:357–63.
[13] Hamilton ML, Van Remmen H, Drake JA, Yang H, Guo ZM, Kewitt K, Walter CA, Richardson A. Does oxidative damage to DNA increase with age? Proc Natl Acad Sci USA 2001;98:10469–74.
[14] Fraga CG, Shigenaga MK, Park JW, Degan P, Ames BN. Oxidative damage to DNA during aging: 8-hydroxy-2′-deoxyguanosine in rat organ DNA and urine. Proc Natl Acad Sci USA 1990;87:4533–7.
[15] Davies SM, Poljak A, Duncan MW, Smythe GA, Murphy MP. Measurements of protein carbonyls, ortho- and meta-tyrosine and oxidative phosphorylation complex activity in mitochondria from young and old rats. Free Radic Biol Med 2001;31:181–90.
[16] Bejma J, Ramires P, Ji LL. Free radical generation and oxidative stress with ageing and exercise: differential effects in the myocardium and liver. Acta Physiol Scand 2000;169:343–51.
[17] Hayashi T, Miyazawa T. Age-associated oxidative damage in microsomal and plasma membrane lipids of rat hepatocytes. Mech Ageing Dev 1998;100:231–42.
[18] Seki S, Kitada T, Sakaguchi H, Nakatani K, Wakasa K. Pathological significance of oxidative cellular damage in human alcoholic liver disease. Histopathology 2003;42:365–71.
[19] Niemela O, Parkkila S, Britton RS, Brunt E, Janney C, Bacon B. Hepatic lipid peroxidation in hereditary hemochromatosis and alcoholic liver injury. J Lab Clin Med 1999;133:451–60.
[20] Kitada T, Seki S, Iwai S, Yamada T, Sakaguchi H, Wakasa K. In situ detection of oxidative DNA damage, 8-hydroxydeoxyguanosine, in chronic human liver disease. J Hepatol 2001;35:613–8.
[21] Devadas S, Zaritskaya L, Rhee SG, Oberley L, Williams MS. Discrete generation of superoxide and hydrogen peroxide by T cell receptor stimulation: selective regulation of mitogen-activated protein kinase activation and fas ligand expression. J Exp Med 2002;195:59–70.

ELSEVIER

International Immunopharmacology 3 (2003) 927–938

International Immunopharmacology

www.elsevier.com/locate/intimp

Role of Fas/Fas ligand-mediated apoptosis in murine contact hypersensitivity

Baohui Xu[a,*], Sivia Bulfone-Paus[b], Kohji Aoyama[a], Su Yu[c], Peixin Huang[d], Kanehisa Morimoto[d], Toshio Matsushita[a,e], Toru Takeuchi[a]

[a] *Department of Environmental Medicine, Faculty of Medicine, Kagoshima University, 8-35-1 Sakuragaoka, Kagoshima 890-8520, Japan*

[b] *Institute of Immunology, Benjamin Franklin Medical Center, Free University Berlin, D-12200 Berlin, Germany*

[c] *Department of Medicine, Stanford University School of Medicine, Stanford, CA 94305, USA*

[d] *Department of Social and Environmental Medicine, Osaka University Graduate School of Medicine, Suita, Osaka, Japan*

[e] *Kagoshima Occupational Health Promotion Center, 6F, I'M. Building, 1-38 Higashisengoku, Kagoshima 892-0842, Japan*

Received 27 December 2002; received in revised form 24 February 2003; accepted 12 March 2003

Abstract

Apoptosis plays an important role in immune responses, but little is known about its involvement in contact hypersensitivity (CH). In this study, we have investigated the role of Fas/Fas ligand (FasL)-mediated apoptosis in the pathogenesis of CH. Mice were sensitized by one topical application of 100 μl of 3% oxazolone to shaved skin of the abdomen. Six days later, CH was provoked by challenging both sides of sensitized mouse right ear with 15 μl of 1% oxazolone. Using a DNA ladder assay, we found that apoptosis was induced in the skin of oxazolone-sensitized mice 24–96 h after allergen challenge. Annexin V-fluorescein isothiocyanate (FITC)-propidium iodide (PI) apoptosis flow cytometric assay showed that early apoptotic $CD4^+$ T cells (annexin V-$FITC^+PI^-$), but not late apoptotic $CD4^+$ T cells (annexin V-$FITC^+PI^+$), increased in the inflamed skin of mice with CH. Moreover, the expressions of mRNAs for T helper (Th2) cytokine (interleukin (IL)-4), Th1 cytokine (interferon (IFN)-γ) and proapoptotic molecules (Bax, Fas, FasL and IL-1β-converting enzyme (ICE)/caspase-1) were significantly elevated in the oxazolone-sensitized mouse skin 6–72 h after allergen challenge. Dramatic increase in IL-10 mRNA was only observed in the sensitized mouse skin 6 and 12 h after allergen challenge. Furthermore, CH was significantly inhibited with decreased apoptosis and early apoptotic $CD4^+$ T cells in inflamed skin in Fas mutant *lpr/lpr* mice compared to wild-type mice, whereas there were no significant differences in IL-4, IFN-γ, IL-10, Bax and ICE mRNAs in the inflamed skin of CH between *lpr/lpr* and wild-type mice. Our results thus suggest that Fas/FasL pathway partially contributes to apoptosis in murine CH and that Fas/FasL-mediated apoptosis plays a partial role in the development of CH. The contribution of Fas/FasL-mediated apoptosis to CH appears independent of Th1 and Th2 cytokines.

Keywords: Mice; Contact hypersensitivity; Apoptosis; Fas; Cytokine

* Corresponding author. Tel.: +81-99-275-5291; fax: +81-99-265-8434.
E-mail address: xubaohui@m.kufm.kagoshima-u.ac.jp (B. Xu).

1567-5769/03/$ - see front matter © 2003 Elsevier Science B.V. All rights reserved.
doi:10.1016/S1567-5769(03)00081-X

1. Introduction

Contact hypersensitivity (CH) is an inflammatory cutaneous disease caused by a cellular immune response to reactive chemicals: $CD4^+$ and $CD8^+$ T cells are involved in the pathogenesis of CH [1–3]. Based on cytokine secretion patterns, $CD4^+$ T cells are classified into two functionally distinct subtypes, Th1 (T helper) and Th2 cells. Th1 cells produce interleukin (IL)-2, interferon (IFN)-γ and tumor necrosis factor (TNF)-α, and contribute to cellular immune responses, while Th2 cells produce IL-4, -5, -6, -10 and -13, and play vital roles in humoral immune responses by helping B-cell antibody production [4]. In CH, Th1 cells in the inflamed skin release cytokines such as IFN-γ and TNF-α. These two Th1 cytokines cause CH by activating macrophages and keratinocytes. Th2 cells are thought to regulate CH by suppressing Th1 cytokine secretion; however, some studies imply that IL-4 is required for the development of CH [1–3,5–8]. It has been shown that modulation of the Th1/Th2 cytokine balance by in vivo neutralization or injection of IL-12 results in suppression or enhancement of CH, respectively [9–12].

Apoptosis, which is mediated by Fas-dependent and Fas-independent pathways, is important in maintaining immune system homeostasis and controlling immune responses [13,14]. In vitro observations suggest that Th1 and Th2 cells undergo apoptosis differentially [15–19]. Th1 and Th2 memory/effector cells develop in draining lymph nodes, enter the bloodstream and migrate to sites of antigen exposure, encounter antigen, become activated and release cytokines such as IL-2, IL-4, IL-10, IFN-γ and TNF-α. However, in vitro data indicate that Th1 and Th2 cytokines exert distinct regulatory role on apoptosis. In this study, we have investigated the roles of Fas/Fas ligand (FasL)-mediated apoptosis in the development of CH.

We found that apoptosis was induced and early apoptotic $CD4^+$ T cells were increased in inflamed skin in CH. Furthermore, both CH and apoptosis were significantly suppressed in functional Fas mutant *lpr/lpr* mice without affecting the levels of Th1 and Th2 cytokine mRNAs in the inflamed skin. These results suggest that apoptosis mediated by the Fas/FasL pathway partially contributes to CH in a Th1 and Th2 cytokine-independent manner.

2. Materials and methods

2.1. Animals

Female BALB/c, wild-type C57BL/6J and functional Fas mutant C57BL/6J *lpr/lpr* mice were purchased from Japan SLC (Hamamatsu, Shizuoka, Japan). Mice were housed in the Institute of Experimental Animal, Faculty of Medicine, Kagoshima University. Eight to 10 age-matched mice (10–12 weeks) were used in each group.

The animal experimental protocol used in this study was approved by the Animal Experimental Committee, Faculty of Medicine, Kagoshima University according to the experimental animal guidelines issued by the Japanese Government and Kagoshima University.

2.2. Provocation of CH to oxazolone

4-Ethyoxymethylene-2-phenyloxazol-5-one (oxazolone, Aldrich Chemical, Milwaukee, WI) was used as the contact allergen. Mice were sensitized by one topical application of 100 μl of 3% oxazolone or equal volume of acetone/olive oil (4:1) to shaved skin of the abdomen. Six days later, baseline ear thickness of both ears for each mouse was measured in triplicate using a dial thickness gauge (Peacock model G, Kawasaki, Japan). Then, both sides of the right ear were challenged with 15 μl of 1% oxazolone, while the left ear was challenged by acetone/olive oil as the control. At different time points after the challenge, the triplicate measurements of ear thickness were made again by the same method. CH to oxazolone is presented as the increase in ear thickness (ear thickness after challenge minus ear thickness before challenge) [20,21].

2.3. Detection of apoptosis

DNA ladder analysis was used to identify apoptosis in the skin. Briefly, control or sensitized mice were sacrificed at different time points after challenge. The ears were excised, cut into small pieces and incubated in the buffer containing 100 μg/ml proteinase K, 100 mM NaCl, 10 mM Tris–HCl (pH 8.0), 25 mM EDTA and 0.5% SDS at 55 °C overnight. Genomic DNA was isolated by phenol/chloroform extraction. Con-

taminating RNA was removed by incubating the samples with RNase H at 37 °C for 1 h. DNA was then extracted with phenol/chloroform, precipitated with ethanol, dried and dissolved in distilled water. Purified DNA (20 μg) was electrophoresed on a 2% agarose gel. The gel was stained in 0.5 μg/ml ethidium bromide solution, viewed on a UV transilluminator and photographed. To compare apoptosis at different time points, the band area for individual DNA fragment was quantified using LabImage Software (Version 2.6, http://www.labimage.de).

Apoptotic $CD4^+$ or $CD8^+$ T cells were analyzed as follows. Ears from control or sensitized mice were cut into small pieces and incubated in Hank's balanced salt solution containing 5% fetal calf serum, 100 units/ml penicillin G, 100 μg/ml streptomycin and 175 units/ml collagenase (Sigma, St. Louis, MO) at 37 °C for 1 h. After being passed through a stainless steel mesh, the lymphocytes were isolated using a mouse lymphocyte separation solution (Japan Antibody Research Institute, Takazaki, Gunnma, Japan). The lymphocytes were stained with Cyc-conjugated anti-CD4 mAb (GK 1.5) or Cyc-conjugated anti-CD8 (55-6.7) (PharMingen, San Diego, CA) followed by annexin V-fluorescein isothiocyanate (FITC) and propidium iodide (PI) (Apoptosis detection kit; MBL, Nagoya, Japan) according to the manufacturer's instructions. The frequency of apoptotic cells was determined using a FACScan cytometer with CellQuest software (Becton Dickinson Immunocytometry System, San Jose, CA).

2.4. Reverse transcription-polymerase chain reaction (RT-PCR)

Ears or draining lymph nodes were excised and stored at −80 °C. RT-PCR analysis of IL-4, IFN-γ, Bax, Bcl-2, Fas, FasL and IL-1β-converting enzyme (ICE)/caspase-1 mRNAs was done as described previously [20–22]. Total RNA was extracted by a guanidinium thiocyanate phenol chloroform isoamyl alcohol procedure. cDNA was synthesized by reverse transcription of total RNA using Moloney Murine Leukemia Virus reverse transcriptase kit (GIBCO BRL) and oligo-dT_{16} primer (Sigma), and amplified by PCR in the presence of gene-specific primers on a MiniCycler (MJ Research, Watertown, MA). PCR cycling conditions were 1 min at 94 °C, 1 min at 60 °C, 2 min at 72 °C, 35 cycles. PCR primers were Bax, sense GCT CTG AAC AGA TCA TGA AGA C, antisense CAT GAT GGT TCT GAT CAG CTC G; Bcl-2, sense TGT GTG TGC AAG TGT AAA TTG C, antisense TCC GCT ACA AGT TAC ACG TTT A; Fas, sense GCT GAT AAA TGC AGA AGA TGC A, antisense ATG CTG TCA TGC ATG ATC TCA T; Fas ligand, sense AAC GAA ACT GGG TTG TAC TTC G, antisense TTC AAG ACA ATA TTC CTG GTG C; ICE/caspase-1, sense GGA CCT ATG TGA TCA TGT CTC T, antisense CTC CTG GAT ACC ATG AGA CAT G; IFN-γ, sense TGA ACG CTA CAC ACT GCA TCT TGG, antisense CGA CTC CTT TTC CGC TTC CTG AG; IL-4, sense ATG GGT CTC AAC CCC CAG CTA GT, antisense GCT CTT TAG GCT TTC CAG GAA GTC; IL-10, sense CCC AGA AAT CAA GGA GCA TTT G, antisense CAT GTA TGC TTC TAT GCA GTT G; GAPDH, sense ACC ACA GTC CAT GCC ATC AC, antisense TCC ACC ACC CTG TTG CTG TA. RT-PCR products were run on a 2% agarose gel, stained in 0.5 μg/ml ethidium bromide solution and imaged using a Gel Image Freezer System (AE6905N, ATTA, Tokyo, Japan). The band area for each RT-PCR product was measured using LabImage software. The relative amount of individual mRNA was calculated as the ratio of the gene of interest to GAPDH.

2.5. Data analysis

Analysis of variance (ANOVA) was used to test the difference between groups. If $p < 0.05$ was obtained in ANOVA, Newman–Keuls test was used to test the difference between two groups. $p < 0.05$ was considered to be significant.

3. Results

3.1. Apoptosis in CH lesions

To determine the kinetics of apoptosis in the inflamed skin of CH, genomic DNA was used for DNA ladder assay. As shown in Fig. 1A, smeared bands with large sizes were observed in DNA from control mouse skin (0 h) or DNA from sensitized mouse skin 6 and 12 h after challenge with 1% oxazolone. In contrast, apoptosis, as characterized

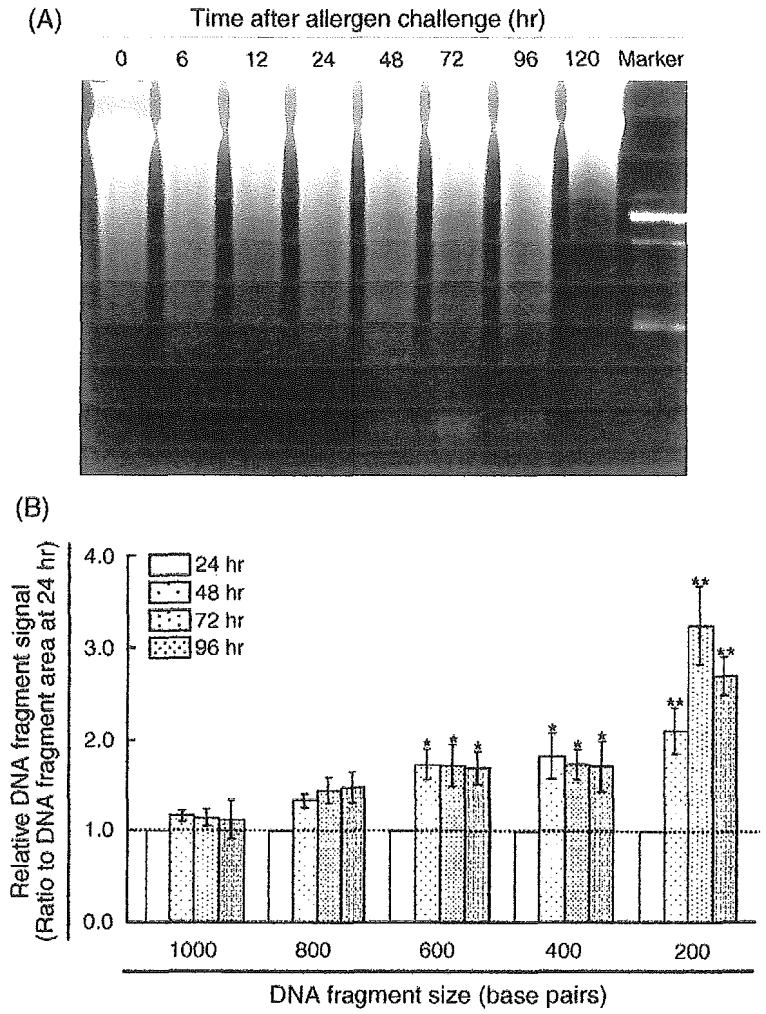

Fig. 1. Apoptosis in the skin of mice with CH. BALB/c mice, sensitized with oxazolone or vehicle, were challenged in the ear with 1% oxazolone. Ears were harvested 6–120 h after challenge. Genomic DNA (20 μg/lane) was used for apoptosis ladder assays. (A) Apoptosis, as characterized by 200, 400, 600, 800 and 1000 bp DNA fragment ladder, was seen in the skin of sensitized mice 24, 48, 72 and 96 h after oxazolone challenge. DNA ladders were not seen in control (0 h) and sensitized mice skin 6, 12 and 120 h after allergen challenge. (B) Ratio of DNA fragment band area to that at 24 h was used as an index of relative DNA fragment signal. The signals for 600, 400 and 200 bp DNA fragments at 48, 72 and 96 h were significantly stronger than those at 24 h. Data are given as mean ± S.D.; *$p<0.05$ at 48, 72 and 96 h for 600 and 400 bp DNA fragments; **$p<0.01$ at 48, 72 and 96 h for 200 bp DNA fragment compared with the ratio (1.0) at 24 h; $n=3$ for each group.

by the appearance of a DNA ladder (200, 400, 600, 800 and 1000 bp DNA fragments), was observed in the skin of sensitized mice 24 h after allergen challenge. Clear DNA ladders were seen at 48–96 h after challenge, but disappeared by 120 h. We found that signals for 600, 400 and 200 bp DNA fragments at 48, 72 and 96 h were significantly stronger than those at 24 h ($p<0.05$ for 600 and 400 bp DNA fragments, $p<0.01$ for 200 bp fragment; the ratio for each fragment at 24 h was set as 1.0) (Fig. 2B). The 200-bp DNA signals at 72 and 96 h were significantly stronger than that at 48 h ($p<0.05$). Using DNA ladder assay, we did not detect apoptosis in the ear skin of sensitized mice that were challenged with acetone/olive oil, or in control mice that were challenged with 1% oxazolone (data not shown).

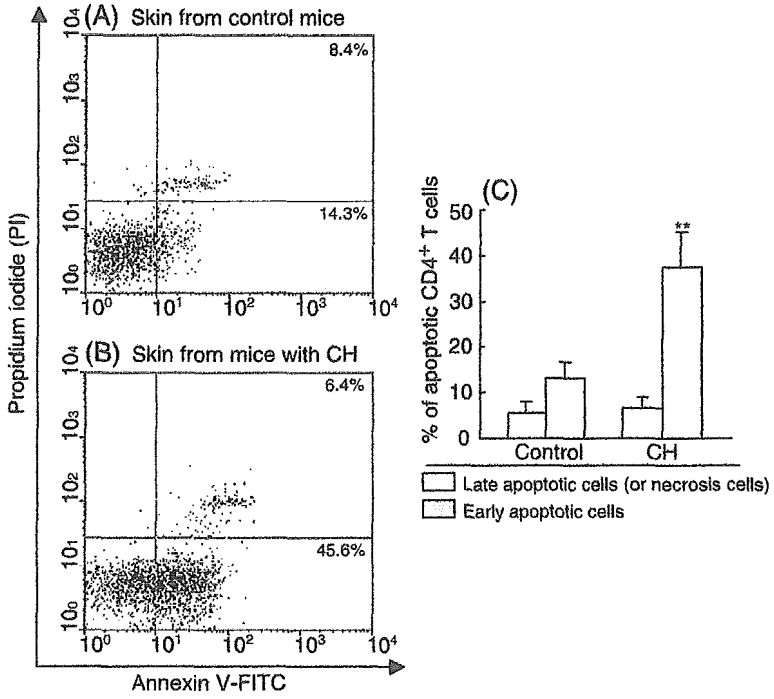

Fig. 2. Apoptotic $CD4^+$ T cells in skin lesions of mice with CH. Lymphocytes were isolated by collagenous digestion from the skin of control or oxazolone-sensitized BALB/c mice 72 h after challenge with 1% oxazolone. The cells were stained with Cyc-CD4, annexin V-FITC and PI. Apoptosis was analyzed by flow cytometry on 5000 gated $CD4^+$ T cells. (A) A representative FACS dot plot shows early apoptotic $CD4^+$ T cells (annexin V-$FITC^+PI^-$, lower right) and late apoptotic $CD4^+$ T cells (annexin V-$FITC^+PI^+$, upper right) in the lymphocytes from control mice ears. (B) A representative FACS dot plot shows an increase in early apoptotic $CD4^+$ T cells (lower right) in the lymphocytes from mice with CH. (C) Data pooled from three experiments show that the percentage of early apoptotic $CD4^+$ T cells in the skin of CH was significantly higher than that in the control mice. Data are given as mean ± S.D. Newman–Keuls test; $^{**}p<0.01$; $n=3-4$ for each group.

Because of the critical roles of $CD4^+$ and $CD8^+$ T cells in CH [1–3,23], we examined whether apoptosis could occur in $CD4^+$ or $CD8^+$ T cells of inflamed skin. For this purpose, lymphocytes were isolated from the ears of sensitized or unsensitized mice 72 h after allergen challenge. Apoptotic $CD4^+$ or $CD8^+$ T cells were analyzed using annexin V-FITC and PI staining. This assay divides apoptotic cells into two stages: early (annexin V-$FITC^+PI^-$) and late (or necrotic) (annexin V-$FITC^+PI^+$). As shown in Fig. 2, both early and late apoptotic $CD4^+$ T cells were seen in the skin of control mice. The percentage of early apoptotic $CD4^+$ T cells in the skin of mice with CH was significantly higher than that in the skin of control mice ($p<0.01$). There was no significant difference in the percentages of late apoptotic $CD4^+$ T cells between the two groups. However, because $CD8^+$ T cells recovered from the control or inflamed mouse skin were extremely limited, we were unable to demonstrate if apoptosis happens to $CD8^+$ T cells at inflamed skin sites.

3.2. Expression of cytokine and apoptosis-related gene mRNAs

Because Th1/Th2 cytokines and apoptosis-related molecules may contribute to apoptosis in CH, we analyzed the time course of expression of Fas, FasL, ICE, Bax, Bcl-2, IL-4 (a representative Th2 cytokine) and IFN-γ (a representative Th1 cytokine) mRNAs in the skin of control mice or mice with CH using semiquantitative RT-PCR.

As shown in Fig. 3, mRNA for IFN-γ, but not for IL-4, was constitutively expressed in control mouse skin (0 h). IL-4 mRNA dramatically increased in the inflamed skin of sensitized mice at 6 h, peaked at 24 h

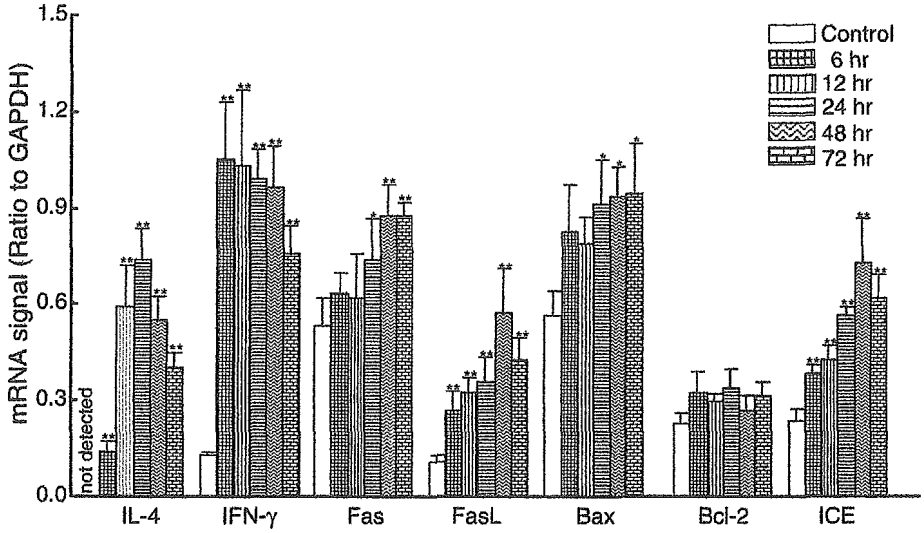

Fig. 3. Expression of cytokine and apoptosis-related gene mRNAs in skin lesions of mice with CH. Total RNA was isolated from the skin of control BALB/c mice or BALB/c mice with CH at different time points. The expression of IL-4, IFN-γ, Fas, FasL, Bax, Bcl-2 and ICE mRNAs was analyzed by semiquantitative RT-PCR. Bax, Fas, FasL, ICE, IL-4 and IFN-γ mRNAs were significantly increased in CH at 6–72 h as compared to control mice. There was no significant difference in Bcl-2 mRNA between groups. Data are given as mean ± S.D. Newman–Keuls test; $*p<0.05$; $**p<0.01$ compared with control group; $n=3$ for each group.

and declined at 48 h after challenge with 1% oxazolone ($p<0.01$ for all time points compared with control mice). The expression of IFN-γ mRNA was significantly enhanced 6–48 h after allergen challenge ($p<0.01$ for all time points compared with control mice). Though IFN-γ mRNA decreased at 72 h, it remained higher than that in control mice ($p<0.01$).

As for proapoptotic and antiapoptotic molecules, Fig. 3 shows that Bax, Bcl-2, ICE/caspase-1, Fas and FasL mRNAs were constitutively expressed in control mice skin. As expected, Fas mRNA was significantly elevated at 24 h and peaked during 48–72 h in the skin of sensitized mice after allergen challenge ($p<0.05$ for 24 h, $p<0.01$ for 48 and 72 h compared with control mice). The expression of FasL and ICE/caspase-1 mRNAs increased remarkably at 6 h, peaked at 48 h and decreased slightly at 72 h ($p<0.01$ for all time points compared with control mice). Bax mRNA was also elevated in the skin of sensitized mice after allergen challenge ($p<0.05$ for 24, 48 and 72 h compared with control mice). However, Bcl-2 mRNA remains unchanged at all time points ($p>0.05$ compared with control mice).

3.3. Impaired CH in lpr/lpr mice lacking Fas-dependent apoptosis

The induction of apoptosis and elevated Fas and FasL mRNAs in the inflamed skin raise the possibility that Fas/FasL-mediated apoptosis may contribute to CH. To address this possibility, we compared CH between wild-type and Fas mutant *lpr/lpr* mice. As shown in Fig. 4, CH was significantly suppressed in sensitized *lpr/lpr* mice during 12–120 h after challenge as compared with wild-type mice (Fig. 4A, $p<0.01$ for 24, 48, 72, 96 and 120 h). Analyzing the mRNA expression of Th1/Th2 cytokines and apoptosis-related molecules in the inflamed skin, we found that mRNA levels for IFN-γ, IL-4, ICE, BAX and Bcl-2 in inflamed skin of *lpr/lpr* mice were similar to those of wild-type mice ($p>0.05$).

3.4. Decreased apoptosis in the inflamed skin of lpr/lpr mice

To determine if decreased CH in *lpr/lpr* mice is associated with changes in apoptosis, we compared apoptosis and apoptotic $CD4^+$ T cells in CH between wild-type and *lpr/lpr* mice at 72 h after challenge.

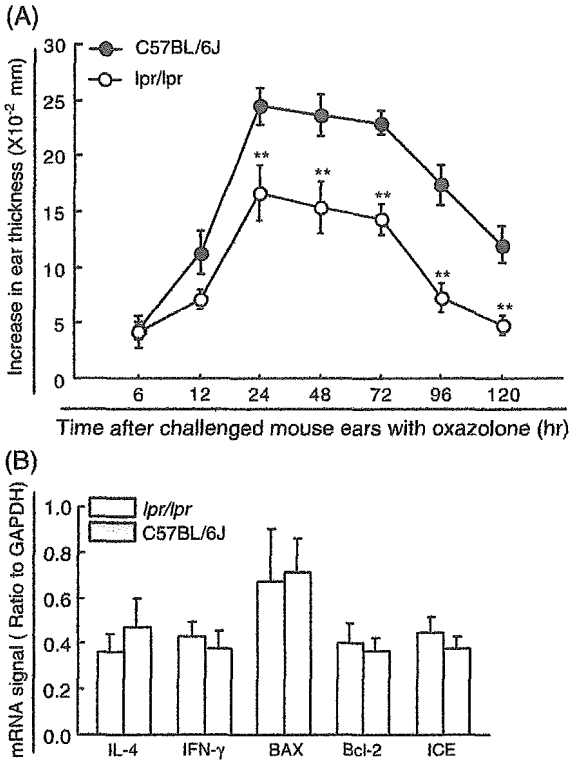

Fig. 4. Impaired CH in *lpr/lpr* mice lacking Fas-dependent apoptosis. (A) CH to oxazolone was suppressed in *lpr/lpr* mice compared to wild-type C57BL/6J mice. $^{**}p<0.01$ compared with C57BL/6J mice at the same time point; $n=5$ for each group. (B) There were no significant differences in the expression of Bax, Bcl-2, ICE, IFN-γ and IL-4 mRNAs in the inflamed skin of CH between *lpr/lpr* and wild-type C57BL/6J mice. ANOVA; $p>0.05$; $n=3-5$ for each group. All data in this figure are given as mean ± S.D.

DNA ladder assay showed that 400 and 200 bp DNA fragments in *lpr/lpr* mice were significantly weaker than those in wild-type mice (Fig. 5A, $p<0.01$ compared with wild-type mice; the wild-type group was set as 100%). However, there were no significant differences for 1000, 800 and 600 bp DNA fragments between *lpr/lpr* and wild-type mice (data not shown for 1000 and 800 bp DNA fragments). Flow cytometric analysis showed that there were fewer $CD4^+$ T cells in lymphocyte preparations from inflamed skin from *lpr/lpr* mice than from wild-type mice (40% for wild-type and 25% for *lpr/lpr* mice). Using annexin V-FITC and PI staining, we found that the percentage of early apoptotic $CD4^+$ T cells in the inflamed skin from *lpr/lpr* mice was significantly lower than that from the wild-type mice (Fig. 5B, $p<0.05$). However, there was no difference in the percentage of late apoptotic $CD4^+$ T cells in the inflamed skin of CH between *lpr/lpr* and wild-type mice.

3.5. Expression of IL-10 mRNA in CH

IL-10 is an important down-regulator in CH and can also be produced by apoptotic T cells [24–27]. To see the relation of IL-10 expression with apoptosis in

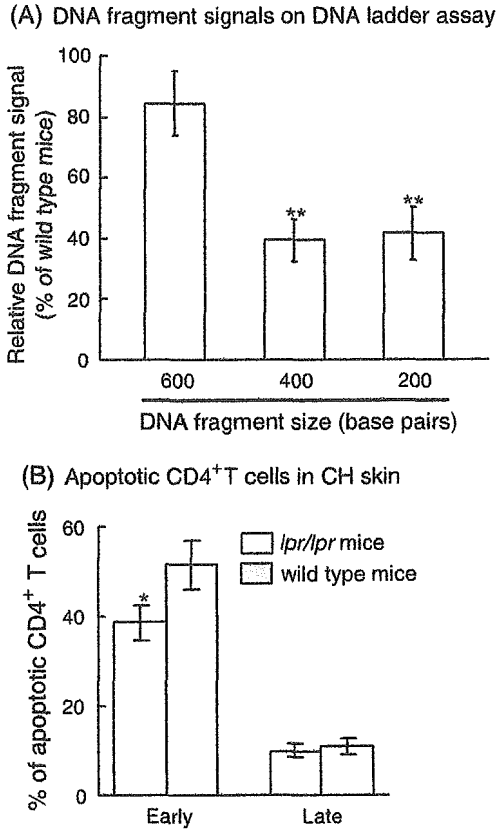

Fig. 5. Decreased apoptosis in the inflamed skin of *lpr/lpr* mice with CH. (A) Genomic DNA from the inflamed skin of *lpr/lpr* and wild-type mice was used for DNA ladder assays. Apoptosis was decreased by 50% in the inflamed skin of *lpr/lpr* as compared to wild-type mice. ANOVA; $p<0.01$ compared with wild-type mice; $n=3$ mice for each group. (B) Lymphocytes were pooled from the inflamed skin of three to four *lpr/lpr* or wild-type mice. Apoptotic cells were analyzed by flow cytometry on gated $CD4^+$ T cells. The percentage of early, but not late, apoptotic $CD4^+$ T cells in the inflamed skin of *lpr/lpr* mice with CH was significantly lower than that in wild-type mice with CH. Newman–Keuls test; $^{**}p<0.05$; $n=3$ mice for each group. All data are mean ± S.D.

CH, we examined the expression kinetics of IL-10 mRNA in the skin of BALB/c with CH. As seen in Fig. 6A, we found that IL-10 mRNA was significantly elevated in the sensitized mouse ear skin 6 and 12 h after challenge with 1% oxazolone ($p<0.01$), but it was almost back to baseline level at 24 h. Compared IL-10 mRNA levels in the draining lymph nodes and skin between *lpr/lpr* and its wild-type control (C57BL/6J) mice, we found that IL-10 mRNA in the draining lymph nodes of wild-type or *lpr/lpr* mice with CH was significantly higher than that in the respective control mice (Fig. 6B, $p<0.01$). However, no significant difference in mRNA levels was seen in the draining lymph nodes of mice with CH between wild-type and *lpr/lpr* mice. Comparable IL-10 mRNA signal was also seen in control or inflamed ear skin between *lpr/lpr* and wild-type mice (Fig. 6C).

4. Discussion

Our study demonstrated that apoptosis was induced in murine CH and at least $CD4^+$ T cells were one type of target cells. We attempted to see if apoptosis could occur in $CD8^+$ T cells. However, we were unable to obtain evidence on the presence or absence of apoptotic $CD8^+$ T cells in the inflamed skin due to limited $CD8^+$ T cell infiltration in the skin of CH. For this reason, we cannot preclude the possibility that $CD8^+$ T cells may become the target. The presence of apoptosis in mouse CH accords with previous human studies. Orteu et al. [28] showed that apoptosis occurred in T cells in sites of CH. Trautmann et al. [29] reported that keratinocytes underwent apoptosis in sites of allergic contact dermatitis or atopic dermatitis. Moreover, we showed here that apoptosis was

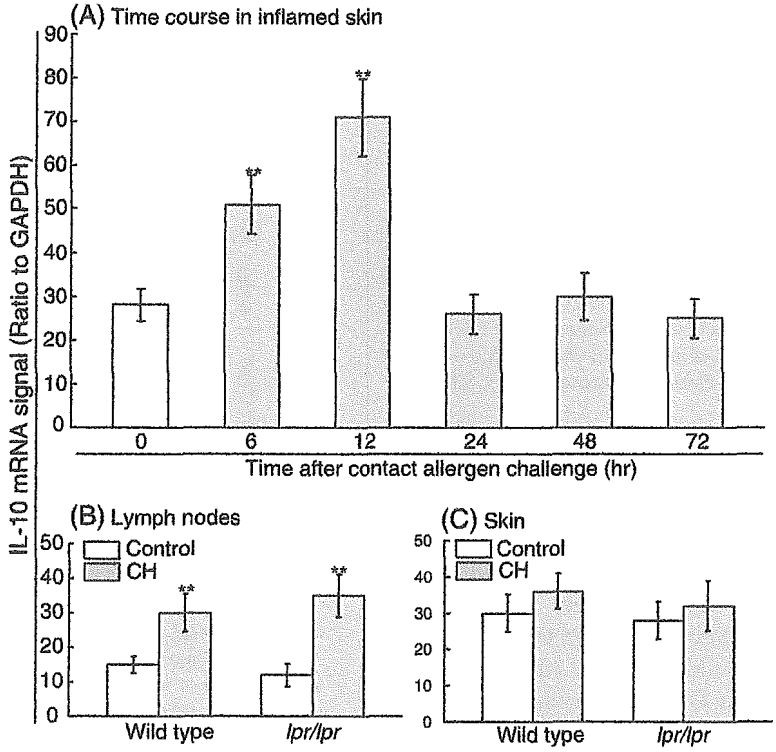

Fig. 6. Expression of IL-10 mRNA in the draining lymph nodes and inflamed skin in murine CH. (A) IL-10 mRNA was only significantly induced in the ear skin of oxazolone-sensitized BALB/c mice 6–12 h but not 24–96 h after challenged with 1% oxazolone. Newman–Keuls test; $^{**}p<0.01$ compared with control mice skin (0 h). (B) Draining lymph nodes from sensitized *lpr/lpr* or sensitized wild-type mice expressed higher IL-10 mRNA compared with the respective control mice (ANOVA; $^{**}p<0.01$), but IL-10 mRNA was similar in the skin of sensitized *lpr/lpr* or sensitized wild-type mice. (C) Inflamed (72 h after allergen challenge) or control mice skin from *lpr/lpr* or wild-type mice expressed comparable IL-10 mRNA. There were three mice in each group. All data are expressed as mean ± S.D.

induced in the skin of sensitized mice 24–96 h after challenge with 1% oxazolone. This time course largely overlapped with the main plateau of CH (24–48 h). Furthermore, we found that CH was significantly impaired in functional Fas mutant *lpr/lpr* mice (about 50% reduction). Consistent with our study, Carlsten et al. [30] showed that contact hypersensitivity was remarkably suppressed in MRL *lpr/lpr* mice. However, Schwarz et al. [31] and Hill et al. [32] reported that mice lacking Fas/FasL pathway (*lpr/lpr* or FasL-deficient *gld/gld* mice) did not alter the development of CH to 2,4-dinitrofluorobenzene (DNFB) or fluorescein isothiocyanate (FITC). Kehren et al. [3] also showed that loss of CH to DNFB was seen unless mice were deficient in both Fas pathway and perforin. Although statistic significance was not seen in two previous reports [31,32], CH to DNFB or FITC tends to be suppressed in *lpr/lpr* or FasL-deficient *gld/gld* mice (about 20–25% reduction) compared with wild-type mice. We noted several differences in the experimental settings in these studies. For example, Schwarz et al. [31] and Hill et al. [32] used *lpr/lpr* or *gld/gld* mice with C3H/H background, while we used *lpr/lpr* with C57BL/6 background. Though Kehren et al. used *lpr/lpr* and *gld/gld* mice with C57BL/6 background, mice used in that study (6 weeks old) were younger than in our study (10–12 weeks old) and others (8–16 weeks old) [30–32]. The difference in the development of CH observed in our studies and previous ones may thus be partly attributed to mouse genetic background and/or age. Additionally, our results are consistent with the functional role of Fas/FasL-mediated apoptosis in other immune diseases such as experimental allergic encephalomyelitis and bleomycin-induced pulmonary fibrosis [33–35]. Taken together, our study suggests that Fas/FasL-mediated apoptosis is in part required for the full development of CH.

Several factors including bacteria, viruses, parasites, cytokines (IFN-γ and TNF) and lymphocyte activation can trigger the Fas/FasL pathway. As reported in previous studies [8,11,22] and this study, lymphocyte activation and its accompanying cytokine production (IFN-γ) occur in the inflamed skin of CH. We propose that lymphocyte activation and/or IFN-γ might act as the activating trigger(s) of the Fas/FasL pathway in CH. Fas and its associated death domain would then form a death-inducing signaling complex. This complex recruits and activates procaspase-8 into caspase-8, which in turn cleaves various cellular proteins such as procaspase-3, which are responsible for cell death [13,14].

Previous in vitro studies have shown that Th1 cells were more susceptible to Fas-dependent apoptosis than Th2 cells, perhaps due to higher expression of FasL or Fas-associated phosphatase by Th1 cells [15–19]. In this study, we showed that apoptosis was induced 24–96 h in the sensitized mouse skin after allergen challenge, while both IFN-γ (Th1) and IL-4 (Th2) mRNAs declined from 48 h in the inflamed skin. These findings imply that, at least in CH, Th1 and Th2 cells may be equally susceptible to Fas-dependent apoptosis. The complex microenvironments surrounding Th1 and Th2 cells in CH might explain the discrepancy between our results and previous in vitro observation. For example, Th1 and Th2 cytokines are expressed in the inflamed skin of CH [11,20–22]. Among these cytokines, IL-2 and IL-4 selectively rescue Th1 and Th2 cells, respectively, from apoptosis [36]. Further, Th1 and Th2 cells coexist with other cells such as naive T cells, neutrophils, macrophages and Langerhans' cells in the inflamed skin. The interaction among Th1 and Th2 cytokines as well as the interaction of Th1/Th2 cells with other infiltrating cells may thus modulate the responses of Th1 and/or Th2 cells to apoptosis.

Moreover, we showed that both CH and apoptosis were inhibited in *lpr/lpr* mice lacking Fas/FasL-mediated apoptosis without affecting the local Th1/Th2 cytokine balance. This disassociation between apoptosis and Th1/Th2 cytokine patterns is in agreement with the significance of apoptosis in other immune diseases. Sabelko et al. reported that experimental allergic encephalomyelitis, a Th1 cells-mediated immune disease, was ameliorated in Fas and/or FasL deficient mice without changes in Th1 and Th2 cytokine profiles [33,34]. Huang et al. [37] showed that there was a strong expression of Th1-related cytokines, IFN-γ and IL-12, in *lpr/lpr* mice infected with the intracellular protozoan *Leishmania major*, but the infection in *lpr/lpr* mice progressed inexorably as compared to wild-type mice. The present study indicates that Fas/FasL-mediated apoptosis may contribute to CH without the involvement of Th1 and Th2 cytokines.

We do not have experimental data to explain how apoptotic cells, particularly $CD4^+$ T cells, contribute to CH. Previous studies showed that IL-10 was induced in skin-resident cells, especially keratinocytes in CH which in turn down-regulated the disease in mice [24–26,38]. Gao et al. [27] further showed that apoptotic T cells produced IL-10 largely in a Fas/FasL-dependent manner. These previous observations imply that, like keratinocytes, apoptotic cells may alter the IL-10 level in our experimental settings. In consistent previous studies, we showed here that increased IL-10 mRNA level was solely seen in the sensitized mouse skin 6–12 h after rechallenge with oxazolone. This time course for IL-10 mRNA expression proceeded earlier than apoptosis which peaked at 24–72 h. Moreover, we did not observe the significant difference in IL-10 mRNA levels in draining lymph nodes and inflamed ear skin of mice with CH between wild-type and *lpr/lpr* mice. Although we did not measure IL-10 protein level, it has been previously shown that the expression of IL-10 mRNA and protein took a similar time course in murine CH [25]. Taken together, our results suggest that apoptotic cells may not produce IL-10 or may produce IL-10 at a level not affected total IL-10 level at inflamed sites or systemically. It is therefore unlikely that IL-10 is involved in suppressed CH in *lpr/lpr* mice. On the other hand, it has been recently shown that apoptotic cells are able to produce other inflammatory mediators and/or chemokines. For example, Matute-Bello et al. [39] reported that activation of the Fas/FasL apoptosis pathway increased polymorphonuclear leukocyte migration into airway spaces and increased TNF-α, IL-6, monocyte chemotactic protein (MCP)-1, macrophage inflammatory protein (MIP)-1α and MIP-2 production by alveolar epithelial cells in mouse lung. Schaub et al. [40] demonstrated that Fas/FasL-mediated apoptosis upregulated the expression of MCP-1 and IL-8 by apoptotic vascular smooth muscle cells in atherosclerotic lesions. Therefore, we assume that apoptotic $CD4^+$ cells might be involved in CH by producing inflammatory mediators other than IL-10 and/or by recruiting other inflammatory cells through chemokine secretion.

We found that ICE/caspase-1 mRNA was significantly elevated in the skin of murine CH. This finding is in agreement with the role of ICE/caspase-1 in CH. Antonopoulos et al. [41] reported that CH was inhibited in either ICE/caspase-1-deficient mice or caspase-1 inhibitor-treated mice. Furthermore, accumulating evidences have suggested that activation of the ICE/caspase cascade is fundamental to Fas/FasL-mediated apoptosis [14,42]. For example, Aiba-Masago et al. [43] showed that caspase-1 acts as an upstream signal to caspase-3 and -9 in Fas-induced apoptotic signaling in rat acinar cells. Takahashi et al. [44] reported that caspase-1 is a downstream signal to caspase-3 and -8 in UV B-induced, Fas-mediated apoptosis in SV40-transformed human keratinocytes. Thus, we speculate that ICE/caspase-1 may be involved in CH by supporting Fas-induced apoptotic signaling.

Although CH was impaired in *lpr/lpr* mice which lack Fas/FasL pathway, apoptosis was only suppressed by about 50% in inflamed skin as compared to wild-type mice. These findings suggest that the Fas/FasL pathway is partially involved in apoptosis in murine CH. In addition, early apoptotic $CD4^+$ T cells were decreased by about 20%. This further suggests that other cells such as $CD8^+$ T cells, macrophages and keratinocytes might also be the targets of Fas/FasL-mediated apoptosis in murine CH. Therefore, the identification of other apoptosis pathways and their target cells may be helpful in further understanding the role of apoptosis in murine CH.

Acknowledgements

This work was supported by grants from a Grant-in-Aid for Scientific Research, the Japanese Ministry of Education, Culture, Sports, Science and Technology (to XBH). We thank Dr. Sara A. Michie for critically reading and improving this manuscript. We also thank Miss Chiko Yumiba for her assistance in this study.

References

[1] Gocinski BL, Tigelaar RE. Roles of $CD4^+$ and $CD8^+$ T cells in murine contact sensitivity revealed by in vivo monoclonal antibody depletion. J Immunol 1990;144:4121–8.

[2] Wang B, Fujisawa H, Zhuang L, Freed I, Howell BG, Shahid S, et al. $CD4^+$ Th1 and $CD8^+$ type 1 cytotoxic T cells both play a crucial role in the full development of contact hypersensitivity. J Immunol 2000;165:6783–90.

[3] Kehren J, Desvignes C, Krasteva M, Ducluzeay MT, Assossou O, Horand F, et al. Cytotoxicity is mandatory for $CD8^+$ T cell-mediated contact hypersensitivity. J Exp Med 1999;189: 779–86.
[4] Abbas AK, Murphy KM, Sher A. Functional diversity of helper T lymphocytes. Nature 1996;383:787–93.
[5] Mohler KM, Butler LD. Differential production of IL-2 and IL-4 mRNA in vivo after primary sensitization. J Immunol 1990;145:1734–9.
[6] Gautam SC, Chikkala NF, Hamilton TA. Anti-inflammatory action of IL-4. Negative regulation of contact sensitivity to trinitrochlorobenzene. J Immunol 1992;148:1411–5.
[7] Asherson GL, Dielli F, Sireci G, Salerno A. Role of IL-4 in delayed type hypersensitivity. Clin Exp Immunol 1996;103: 1–4.
[8] Ohmen JD, Hanitifin JM, Nickoloff BJ, Rea TH, Wyzykowski R, Kim J, et al. Overexpression of IL-10 in atopic dermatitis. Contrasting cytokine patterns with delayed-type hypersensitivity reactions. J Immunol 1995;154:1956–63.
[9] Riemann H, Schwarz A, Grabbe S, Aragane Y, Luger TA, Wysocka M, et al. Neutralization of IL-12 in vivo prevents induction of contact hypersensitivity and induces hapten-specific tolerance. J Immunol 1996;156:1799–803.
[10] Muller G, Saloga J, Germann T, Schuler G, Knop J, Enk AH. IL-12 as mediator and adjuvant for the induction of contact sensitivity in vivo. J Immunol 1995;155:4661–8.
[11] Xu BH, Aoyama K, Kitani A, Yu S, Matsuyama T, Matsushita T. Interleukin-12 enhances contact hypersensitivity by modulating the in vivo cytokine pattern in mice. J Interferon Cytokine Res 1998;18:23–31.
[12] Yokozeki H, Ghoreishi M, Takagawa S, Takayama K, Satoh T, Katayama I, et al. Signal transducer and activator of transcription 6 is essential in the induction of contact hypersensitivity. J Exp Med 2000;191:995–1004.
[13] Nagata S. Apoptosis by death factor. Cell 1997;88:355–65.
[14] Krammer PH. CD95's deadly mission in the immune system. Nature 2000;407:789–95.
[15] Zhang X, Brunner T, Carter L, Dutton RW, Rogers P, Bradley L, et al. Unequal death in T helper cell (Th)1 and Th2 effectors: Th1, but not Th2, effectors undergo rapid Fas/FasL-mediated apoptosis. J Exp Med 1997;185: 1837–49.
[16] Varadhachary AS, Perdow SN, Hu C, Ramanarayanan M, Salgame P. Differential ability of T cell subsets to undergo activation-induced cell death. Proc Natl Acad Sci U S A 1997;94:5778–83.
[17] Vandenbark AA, Barnes D, Finn T, Bourdette DN, Whitham R, Robey I, et al. Differential susceptibility of human T(h)1 versus T(h)2 cells to induction of energy and apoptosis by ECDI/antigen-coupled antigen-presenting cells. Int Immunol 2000;12:57–66.
[18] Ramsdell F, Seaman MS, Miller RE, Picha KS, Kennedy MK, Lynch DH. Differential ability of Th1 and Th2 T cells to express Fas ligand and to undergo activation-induced cell death. Int Immunol 1994;6:1545–53.
[19] Oberg HH, Lengl-Janssen B, Kabelitz D, Janssen O. Activation-induced T cell death: resistance or susceptibility correlate with cell surface fas ligand expression and T helper phenotype. Cell Immunol 1997;181:93–100.
[20] Xu BH, Aoyama K, Kitani A, Matsuyama T, Matsushita T. Expression of cytokine mRNAs in the draining lymph nodes following contact in mice. Toxicol Methods 1997;7:137–48.
[21] Xu BH, Aoyama K, Yu S, Kitani A, Okamura H, Kurimoto M, et al. Expression of interleukin-18 in murine contact hypersensitivity. J Interferon Cytokine Res 1998;18:653–9.
[22] Xu BH, Aoyama K, Kitani A, Matsuyama T, Matsushita T. RT-PCR analysis of in vivo cytokine profiles in murine allergic contact dermatitis to DNCB. Toxicol Methods 1996;6: 23–31.
[23] Hauser C. Cultural epidermal Langerhans cells activate effector T cells for contact hypersensitivity. J Invest Dermatol 1990; 95:436–40.
[24] Rivas JM, Ullrich SE. Systemic suppression of delayed type hypersensitivity by supernatants from UV-irradiated keratinocytes: an essential role for keratinocyte-derived IL-10. J Immunol 1992;149:3865–71.
[25] Ferguson TA, Dube P, Griffith TA. Regulation of contact hypersensitivity by interleukin 10. J Exp Med 1994;179: 1579–604.
[26] Berg DJ, Leach MW, Kuhn R, Rajewsky K, Muller W, Davidson NJ, et al. Interleukin 10 but not interleukin 4 is a natural suppressant of cutaneous inflammatory responses. J Exp Med 1995;182:99–108.
[27] Gao YK, Herndon JM, Zhang W, Griffith TS, Feruson TA. Antiinflammatory effects of CD95 ligand (FasL)-induced apoptosis. J Exp Med 1998;188:887–96.
[28] Orteu CH, Poulter LW, Rustin MH, Sabin CA, Salmon M, Akbar AN. The role of apoptosis in the resolution of T cell-mediated cutaneous inflammation. J Immunol 1998;161: 1619–29.
[29] Trautmann A, Akidis M, Kleemann D, Altznauer F, Simon H, Graeve T, et al. T cell-mediated Fas-induced keratinocyte apoptosis plays a key pathogenetic role in eczematous dermatitis. J Clin Invest 2001;106:25–35.
[30] Carlsten H, Tarkowski A, Nilsson LA. The effect of immunomodulating treatment on cutaneous delayed type hypersensitivity in MRL *lpr/lpr* mice. APMIS 1989;97:728–32.
[31] Schwarz A, Grabbe S, Grosse-Heitmeyer K, Roters B, Riemann H, Luger TA, et al. Ultraviolet light-induced immune tolerance is mediated via the Fas/Fas-ligand system. J Immunol 1998;160:4262–70.
[32] Hill LL, Shreedhar VK, Kripke ML, Owen-Schaub LB. A critical role for Fas ligand in the active suppression of systemic immune responses by ultraviolet radiation. J Exp Med 1999;189:1285–93.
[33] Sabelko KA, Kelly KA, Nahm MH, Cross AH, Russell JH. Fas and Fas ligand enhance the pathogenesis of experimental allergic encephalomyelitis, but are not essential for immune privilege in the central nervous system. J Immunol 1997; 159: 3096–9.
[34] Waldner H, Sobel RA, Howard E, Kuchroo VK. Fas- and FasL-deficient mice are resistant to induction of autoimmune encephalomyelitis. J Immunol 1997;159:3100–3.
[35] Kuwano K, Hagimoto N, Kawasaki M, Yatomi T, Nakamura

N, Nagata S, et al. Essential roles of the Fas–Fas ligand pathway in the development of pulmonary fibrosis. J Clin Invest 1999;104:13–9.
[36] Zubiaga AM, Munoz E, Huber BT. IL-4 and IL-2 selectively rescue Th cell subsets from glucocorticoid-induced apoptosis. J Immunol 1992;149:107–12.
[37] Huang FP, Xu D, Esfandiari EO, Sands W, Wei XQ, Liew FY. Mice defective in Fas are highly susceptible to *Leishmania major* infection despite elevated IL-12 synthesis, strong Th1 responses, and enhanced nitric oxide production. J Immunol 1998;160:4143–7.
[38] Enk AH, Katz SI. Identification and induction of keratinocyte-derived IL-10. J Immunol 1992;149:92–5.
[39] Matute-Bello G, Winn RK, Jonas M, Chi EY, Martin TR, Liles WC. Fas (CD95) induces alveolar epithelial cell apoptosis in vivo. Implications for acute pulmonary inflammation. Am J Pathol 2001;158:153–61.
[40] Schaub FJ, Han DKM, Liles WC, Adams LD, Coats SA, Ramachandran RK, et al. Fas/FADD-mediated activation of a specific program of inflammatory gene expression in vascular smooth muscle cells. Nat Med 2000;6:790–6.
[41] Antonopoulos C, Cumberbatch M, Dearman RJ, Daniel RJ, Kimber I, Groves RW. Functional caspase-1 is required for Langerhans cell migration and optimal contact sensitization in mice. J Immunol 2001;166:3672–7.
[42] Henkart P. ICE family proteases: mediators of all apoptotic cell death? Immunity 1996;4:195–201.
[43] Aiba-Masago S, Masago R, Vela-Roch N, Talal N, Dang H. Fas-mediated apoptosis in a rat acinar cell line is dependent on caspase-1 activity. Cell Signal 2001;9:17–24.
[44] Takahashi H, Nakamura S, Asano K, Kinouchi M, Ishida-Yamamoto A, Iizuka H. Fas antigen modulates ultraviolet B-induced apoptosis of SVHK cells: sequential activation of caspase 8, 3, and 1 in the apoptotic process. Exp Cell Res 1999;249:291–8.

ACADEMIC PRESS

Available online at www.sciencedirect.com

SCIENCE DIRECT®

Biochemical and Biophysical Research Communications 304 (2003) 619–624

BBRC

www.elsevier.com/locate/ybbrc

Method to overcome photoreaction, a serious drawback to the use of dichlorofluorescin in evaluation of reactive oxygen species

Muhammad Afzal,[a] Seiichi Matsugo,[b] Masaaki Sasai,[b] Baohui Xu,[a] Kohji Aoyama,[a] and Toru Takeuchi[a,*]

[a] *Department of Environmental Medicine and Hygiene, Kagoshima University Faculty of Medicine, 8-35-1 Sakuragaoka, Kagoshima 890-8520, Japan*

[b] *Department of Applied Chemistry and Biotechnology, Faculty of Engineering, University of Yamanashi, 4-3-11 Takeda, Kofu 400-8511, Japan*

Received 13 March 2003

Abstract

Non-fluorescent dichlorofluorescin (DCFH) was converted to fluorescent products by photo-irradiation during observations with spectrofluorometer and fluorescence microscopy. Photo-irradiation of DCFH at 250, 300, 330, 400, 500, or 600 nm generated fluorescent dichlorofluorescein (DCF), an oxidation product of DCFH, and an unrecognized fluorescent product. The ratio of the unknown product to DCF varied from 0.15 to 8.21 depending on wavelength. Although reactive oxygen species scavengers, such as catalase, superoxide dismutase, and sodium azide, did not suppress the increase in non-specified fluorescence, reagents such as ascorbic acid, mercaptopropionyl glycine, and methoxycinnamic acid, in a cell-free system, almost completely suppressed it with little effect on the fluorescence of DCF. Meanwhile, ascorbic acid also suppressed non-specified fluorescence in cells, but not completely. At low concentrations of DCFH, the speed of increasing fluorescence was considerably retarded, to such a degree that the fluorescence increase in cells during fluorescence microscopic observation was negligible. The addition, at the time of evaluation, of the above reagents to cell-free systems and, in cell systems, reducing the concentration of DCFH, effectively suppressed the photoreaction of DCFH.

Keywords: Dichlorofluorescein; Dichlorofluorescin; Fluorescence microscopy; HL60 cell; Photo-oxidation; Photoreaction; Reactive oxygen species; Spectrofluorometer

DCFH-DA (dichlorofluorescin–diacetate) is widely used for the analysis of reactive oxygen species (ROS) in cells [1–4]. DCFH-DA is converted to DCFH by intracellular esterases and non-fluorescent DCFH is oxidized to DCF (fluorescent dichlorofluorescein) by reaction with ROS. Thus, increasing fluorescence may be a useful indicator of increased ROS generation. Recent reports, however, show that DCFH is oxidized in processes that do not involve ROS [5–7]. Meanwhile, photo-irradiation incidental to spectrofluorometric or fluorescence microscopic observation has also been reported to oxidize DCFH [8–11]. Photo-oxidation is a serious problem for the use of DCFH as an indicator because photo-irradiation is necessary to determine the fluorescence of DCF in the presence of DCFH. Thus, some studies suggest that photo-oxidation makes it difficult [11] or even impossible [10] to quantitatively analyze the generation of ROS with DCFH. On the other hand, because DCFH is highly sensitive to ROS, widely available, and easy to use, it has great potential as a reagent for studying ROS generation. Were it possible to suppress the photo-oxidation of DCFH during analytic processes, DCFH would be a more reliable fluorescent probe for ROS. Despite the drawbacks, the photo-oxidation of DCFH has not been well studied, neither have any reports described how to suppress the photo-oxidation of DCFH.

During fluorescence microscopy we had observed a rapid increase in the fluorescence intensity of DCFH-loaded cells that made it impossible to distinguish differences in fluorescence between ROS-generating cells

* Corresponding author. Fax: +81-99-265-8434.
E-mail address: takeuchi@m.kufm.kagoshima-u.ac.jp (T. Takeuchi).

0006-291X/03/$ - see front matter © 2003 Elsevier Science (USA). All rights reserved.
doi:10.1016/S0006-291X(03)00641-7

and ROS non-generating cells. The aim of the present study was to investigate the photo-reactivity of DCFH and find a way to ensure the reliability of DCFH for ROS evaluation.

Materials and methods

Materials. DCFH-DA was purchased from Molecular Probe (Eugene, OR), dissolved in dimethyl sulfoxide (DMSO) at 5 mM, and stored, protected from light, at −80 °C. DCF-DA was purchased from Fluka Chemie GmbH (Buchs, Switzerland), prepared, and similarly stored. Esterase and cytochrome *c* were purchased from Sigma–Aldrich (Tokyo, Japan). Esterase was dissolved in water at 200 U/ml and stored at 4 °C. HL60 cells were obtained from Japan Cancer Research Resources Bank, and grown with RPMI 1640 containing 10% heat-inactivated fetal calf serum (medium) as described elsewhere [12]. HL60 cells were differentiated with medium containing 1.3% DMSO (DMSO-HL60) during 4 days. When evaluated with cytochrome *c*, these DMSO-HL60 cells generated O_2^- at 1–2.2 μM/2.5 × 10^6/ml/min, i.e., four to eight times less than 7 days-differentiated DMSO-HL60 or human neutrophils [12].

VC (ascorbic acid), Na azide (sodium azide), MC (methoxycinnamic acid), and SOD (Cu–Zn superoxide dismutase) were purchased from Wako Pure Chemical Industries (Osaka, Japan); catalase was purchased from Boehringer–Mannheim (Mannheim, Germany); and MPG (mercaptopropionyl glycine) was purchased from Sigma–Aldrich (Tokyo, Japan). In cell-free experiments, VC, Na azide, and MPG were dissolved in DPBS (Dulbecco's phosphate-buffered saline). In cell experiments, VC and MPG were dissolved in HBSS–Hepes (Hanks' balanced salt solution with 20 mM Hepes–NaOH, pH 7.4). MC was dissolved in DMSO; both were freshly prepared.

Preparation of DCFH and DCF. DCFH was prepared from DCFH-DA (5 μM) after incubation with esterase (1 U/ml) in DPBS for 15 min at 37 °C. DCF was similarly prepared from DCF-DA.

Anaerobic preparation of DCFH. DCFH-DA was hydrolyzed with esterase as described above in an anaerobic incubator [13]. Then, in the anaerobic conditions, DCFH was diluted in cuvettes to 0.25 μM with DPBS. In the anaerobic incubator, the cuvettes were tightly sealed with glass caps and parafilm. Before use, the DPBS had been allowed to stand in the incubator for more than 24 h.

Photo-irradiation of DCFH. DCFH was diluted with DPBS to 0.25 μM and, at room temperature, continuously irradiated at the indicated wavelength with a 150 W xenon lamp for excitation in a JASCO FP-750 spectrofluorometer (Tokyo, Japan).

The pH values of the reaction mixtures were adjusted with HCl or NaOH and measured using a pH meter (Corning Scholar 425; New York, NY).

Measurements of fluorescence. Fluorescence of photo-irradiated DCFH or DCF was measured using the JASCO FP-750 spectrofluorometer with excitation wavelength set at 500 nm and emission at 520 nm.

Identification of fluorescent products by HPLC. Photo-irradiated DCFH samples were separated and fluorescent products were evaluated using a HPLC system. The samples were put into an ODS-80Ts column (4.6 × 150 mm; TOSOH, Japan), eluted at 0.8 ml/min with 0.1 M sodium phosphate (pH 7.4):acetonitrile/5:1, and then detected fluorometrically with excitation and emission wavelengths set at 500 and 520 nm.

Preparation of DCFH-loaded cells. DMSO-HL60 cells were washed and suspended in HBSS–Hepes at 2.5 × 10^6/ml. The cells were incubated with DCFH-DA (5 or 0.25 μM) at 37 °C for 10 min and then stimulated for 15 min with or without 1.0 μM PMA (phorbol myristate acetate) at 37 °C. In some experiments VC and NaOH were added to the cells after the stimulation and the cells were incubated at 0 °C for 150 min.

Fluorescence microscopic observation of the cells. Fluorescence intensities of the DCFH-loaded cells were observed with a Carl Zeiss Axioskop 40 fitted with an Omega Optical XF22 filter set (Jena, Germany) and a Leistungselektronik mbq 52 ac (Jena, Germany), which was equipped with an HBO50 mercury lamp. During the observation the cells were continuously irradiated with excitation light. Images were captured with a Pixera Penguin 150CL digital camera and Pixera Viewfinder 3.0 (Los Gatos, CA) with sensitivity set at 50 and exposure at 1/5 s or 1/2 s.

Statistical analyses. Statistical differences between groups was determined by Student's *t* test. *P* values <0.01 were considered significant.

Results and discussion

Results during spectrofluorometer observation indicated that DCFH was converted to fluorescent compounds (Fig. 1). Based on all previous reports, which have assumed that DCFH is photo-oxidized to DCF [8–10], we similarly assumed that all the increase in fluorescence was due to the formation of DCF and calculated that 4.2 ± 1.0% of DCFH was photo-oxidized to DCF after 90 s of 500 nm irradiation. When we tried to identify the fluorescent products with HPLC, however, we detected two fluorescent peaks (Fig. 2). More than 99% of fluorescence was recovered in the two peaks. This finding is the first report to show that DCF is not the only fluorescent product resulting from DCFH convertion. The second fluorescent peak (P2) could be identified as DCF (Fig. 2A) because it had the same elution time and co-eluted with DCF. We are still trying to determine the compound responsible for the first fluorescent peak (P1). Depending on the wavelength of irradiation, the ratio of unknown substance to DCF varied from 0.15 to 8.21; at 300 nm the ratio was 8.21 (Fig. 2D), whereas at 400 nm the ratio was 0.15 (Fig. 2C); at 500 nm it was 1.5 (Fig. 2B). The focus of the present report is how to suppress the photoreaction of

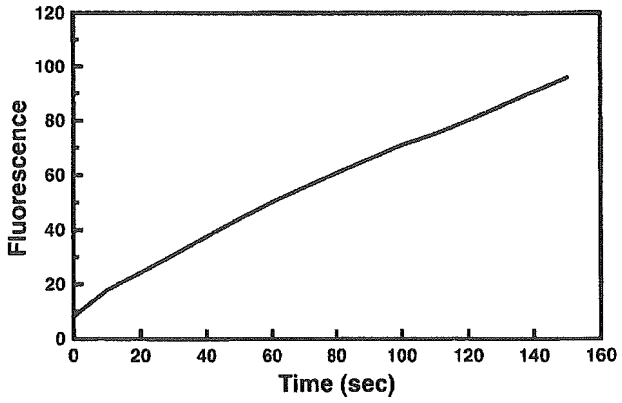

Fig. 1. Photoreaction of DCFH. DCFH was continuously irradiated at 500 nm with a 150 W xenon lamp in a FP-750 spectrofluorometer. The fluorescence of the irradiated sample was measured at wavelengths of 500 nm for excitation and for 520 nm emission.

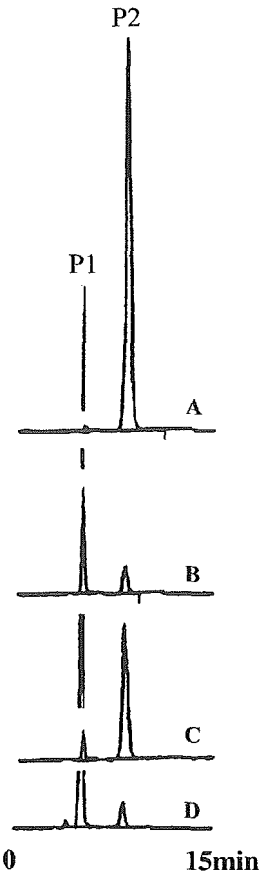

Fig. 2. Elution profile of photo-irradiated DCFH. Samples of DCF (A) or photo-irradiated DCFH (B–D) were put in an ODS-80Ts column (4.6 × 150 mm), eluted with 0.1 M sodium phosphate:acetonitrile/5:1, and then fluorometrically evaluated at wavelengths of 500 nm for excitation and 520 nm for emission. For 90 s, DCFH was irradiated at 500 (B), 400 (C), or 300 nm (D). DCF (P2) and an unknown product (P1) were detected in the irradiated samples; the ratio of the unknown substance to DCF differed considerably depending on the irradiation wavelength.

DCFH; when we identify and elucidate the mechanism of formation of the unknown product we will issue a separate report.

The photoreactivity of DCFH was the most prominent when DCFH was irradiated at 300 nm (Fig. 3); DCFH has an absorption band around 300 nm, so irradiation in this region of the spectrum may stimulate DCFH to produce fluorescent compounds. Even so, irradiation at any wavelength tested up to now, including wavelengths normally used for the excitation of DCF, increases fluorescence from DCFH. We still do not know why irradiation at wavelengths outside the absorption band induce DCFH photoreactivity or why the ratio of photoreaction products varied according to the irradiation wavelength.

Although the addition of catalase or elimination of oxygen had little effect on the photoreactivity of DCFH, SOD or Na azide enhanced photoreaction (Fig. 4).

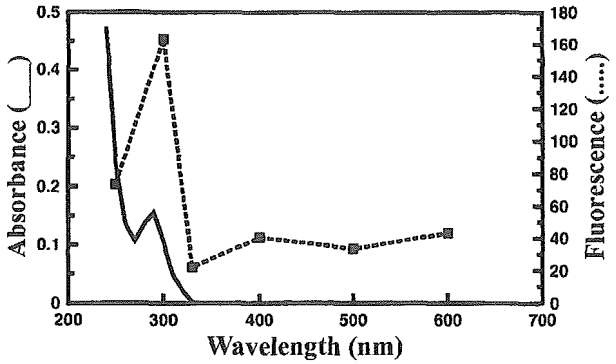

Fig. 3. Absorption and action spectra of DCFH. The solid line indicates the absorption spectrum of DCFH. After irradiation with a 150 W xenon lamp at the indicated wavelengths for 90 s, the fluorescence (dotted line) of photo-irradiated DCFH was measured with wavelengths of 500 nm for excitation and 520 nm for emission. Fluorescence data were averaged from the results of four experiments.

These results indicate that neither H_2O_2, $^1O_2$, nor $O_2^{\cdot-}$ was involved in these DCFH photo-reactions; nor were ROS scavengers able to suppress the photoreaction. This enhancement of DCFH photoreaction with SOD or Na azide corroborates previous findings [9,14,15]. The addition of H_2O_2 had little effect on the photoreaction and co-addition of catalase with SOD did not suppress SOD-enhanced DCFH photo-reactivity (data not shown). When DCFH was oxidized with H_2O_2 and horseradish peroxidase, the ratio of the unknown substance (P1) to DCF (P2) was 0.05 (data not shown).

Varying the level of pH considerably affected both the DCF fluorescence and DCFH photoreactivity. Acidity suppressed DCFH photoreactivity more than DCF flu-

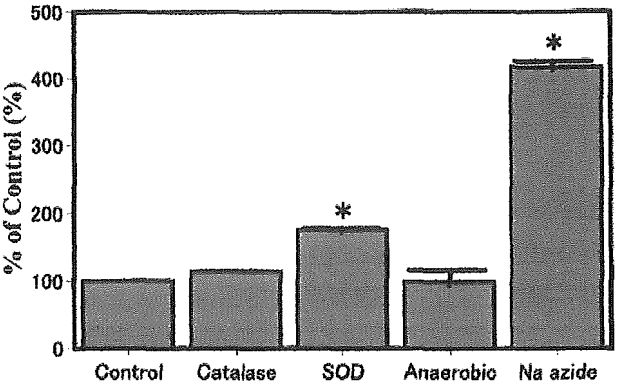

Fig. 4. Effects of ROS scavengers on photoreaction of DCFH. After irradiation for 90 s at 500 nm with a 150 W xenon lamp in the absence (control) or presence of ROS scavengers, the fluorescence intensities of irradiated DCFH samples were measured with wavelengths of 500 nm for excitation and 520 nm for emission. Concentrations of ROS scavengers were 500 U/ml catalase, 500 U/ml SOD, and 10 mM Na azide. 'Anaerobic' means that the DCFH solution was prepared in an anaerobic incubator, tightly sealed, and then irradiated as above. Data were averaged from the results of four to six experiments. The line bars indicate SE. *Significantly different to control.

orescence (Fig. 5), indicating that the protonated form of DCFH is more less liable to photoreaction (Fig. 7). At around pH 6.5, the photoreaction was reduced to 50%, which corresponds well with pK_a 6.4 of DCFH (data from Molecular Probe).

VC, MPG, or MC almost completely suppressed the photoreactivity of DCFH with little effect on the fluorescence of DCF. In these experiments we used NaOH to adjust pH values to between 7.2 and 7.5 (Fig. 6). Bilski et al. [9] have reported that VC increases the photosensitized oxidation of DCFH. We found that the suppressive effects of VC were concentration dependent, however, at lower concentrations, such as 0.25 or 1.0 μM, VC did not enhance photoreactivity in our system (data not shown). This discrepancy in the findings could be because our protocol did not include photosensitizer. VC, MPG, or MC could be used to suppress photoreaction of DCFH in cell-free experiments because they did not reduce DCF fluorescence.

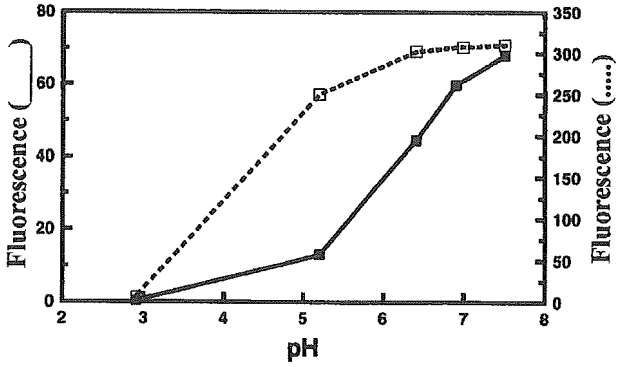

Fig. 5. Effects of pH on photoreaction of DCFH and fluorescence of DCF. After irradiation for 90 s at 500 nm with a 150 W xenon lamp and fluorescence intensities of irradiated DCFH (solid line) samples at the indicated pH values were measured with wavelengths of 500 nm for excitation and 520 nm for emission. Fluorescence of DCF (dotted line) at the indicated pH values was measured as described above. Data were averaged from the results of two independent experiments.

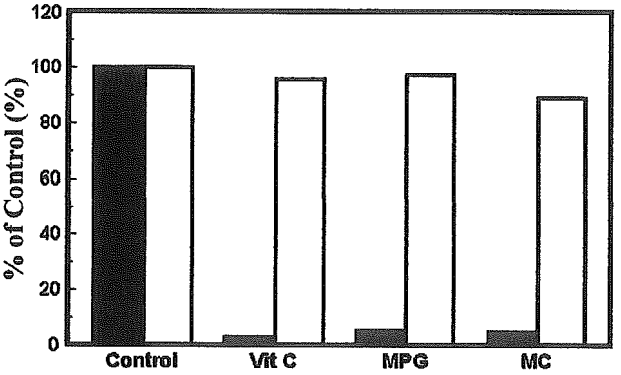

Fig. 6. Effects of antioxidants on photoreaction of DCFH and fluorescence of DCF. After irradiation, in the absence (control) or presence of antioxidants, for 90 s at 500 nm with a 150 W xenon lamp, the fluorescence intensities of irradiated DCFH (solid bars) samples were measured with wavelengths of 500 nm for excitation and 520 nm for emission. Fluorescence of DCF (open bars) in the absence (control) or presence of antioxidants was measured as described above. Concentrations of antioxidants were 10 mM VC, 10 mM MPG, and 5 mM MC. Data were averaged from the results of two independent experiments.

We illustrate the likely mechanism of DCFH photooxidation in Fig. 7. Photo-irradiation gives rise to the formation of 2* (excited state of 2), which smoothly abstracts the hydrogen atom at the 9-position of 1 to afford 3 and 4. The transfer of an electron from 4 to oxygen affords superoxide and 1. Meanwhile, the same reaction also takes place in 3 and affords superoxide and 5. Deprotonation of 5 affords DCF as the final product. The addition of VC, MPG, or MC can inhibit the hydrogen abstraction process of 2* by competing with 1, which decreases the formation of 3. Rota et al. [6] have reported the formation of 3 and we have confirmed the formation of $O_2^{\cdot-}$ during photo-irradiation of DCFH. When we irradiated DCFH at 400 nm, 87.2%, and at 500 nm, 38.2%, of fluorescence increase was due to DCF (Figs. 2B and C). Because excitation in the range of 400–500 nm is the most commonly used wavelength for DCF evaluation, mechanism that we suggest above seems to play a major role in the photoreaction of DCFH.

The fluorescence intensity of unstimulated DMSO-HL60cells increased rapidly during fluorescence microscopic observation (Fig. 8A–). Immediately after commencement of fluorescence microscopic observation (0 s), values were less than those of stimulated DMSO-HL60 cells, but values for unstimulated and stimulated cells became similar after 10 s of continuous observation (Fig. 8A). In a previous study with a confocal laser-scanning microscope we had experienced similar difficulties [4]. Because VC was the most effective of the suppressants we tested, we evaluated the effects of VC on the photoreactivity of DCFH in cells. After 150 min incubation, 50 mM of VC at pH 5.0 suppressed the cellular photoreaction of DCFH (Fig. 8B–). VC also suppressed the increase of extracellular fluorescence and yielded clearer fluorescence images of cells (Fig. 8B). Although VC always suppressed the photoreaction in cells, the suppression was never complete and varied from experiment to experiment. At pH 7.4, VC suppressed only the extracellular, not intracellular, photoreaction of DCFH; thus VC should be used in acidic conditions.

Suppression of the photoreaction of DCFH within cells may depend on the intracellular concentration of VC and may vary according to the cell conditions. A long incubation time with VC, such as 150 min, seems necessary to achieve an intracellular concentration of VC sufficient to suppress photoreaction. Variation between experiments and long incubation time were shortcomings of this method of suppression. We lowered the concentration of DCFH to see if considerably

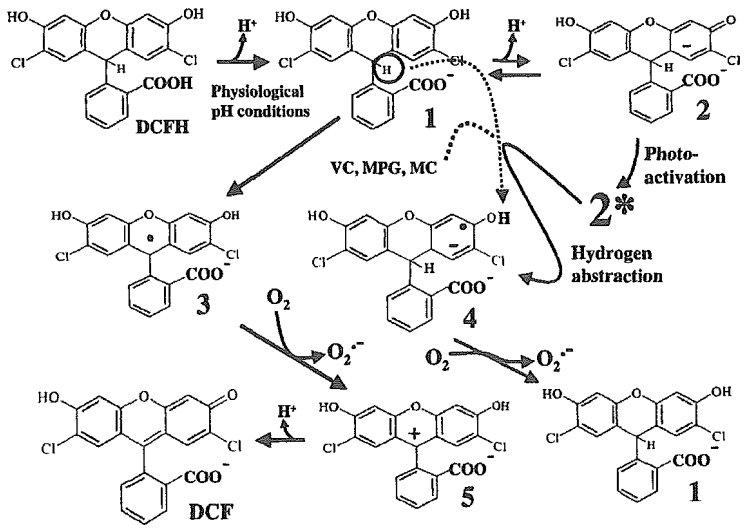

Fig. 7. Mechanism of photo-oxidation of DCFH.

lower concentrations of VC would be sufficient to suppress photoreaction. If so, it might be feasible to reduce the incubation time and get better suppression with the same concentration of VC. When we reduced DCFH concentration to 0.25 μM, cellular photoreaction of DCFH was hardly detectable, even in the absence of VC (Fig. 8C–). The difference in fluorescence intensity between stimulated and unstimulated cells was clearly apparent (Fig. 8C), even with less differentiated HL60 cells which generated ROS four to eight times less actively than fully differentiated HL60 cells or neutrophils [12]. The effect of catalase, which suppressed fluorescence intensities in PMA stimulated cells, was also evident (data not shown). Although the increase was too slight to be recorded by our capture equipment, in samples prepared with 0.25 μM DCFH, a faint and slow increase in fluorescence during microscopic observation was visually perceptible. VC enabled further suppression of photoreaction (data not shown).

In a cell-free system, we confirmed that the speed of photoreaction of DCFH was dependent on DCFH concentration (Fig. 9). When we decreased the concentration of DCFH to 0.25 μM the speed of the DCFH

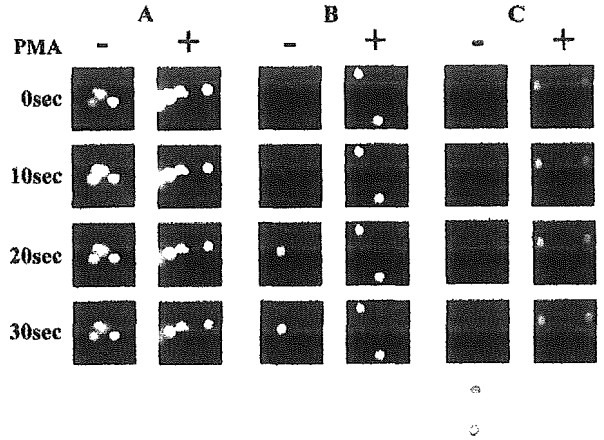

Fig. 8. Photoreaction of DCFH in DMSO-HL60. DMSO differentiated HL60 cells (DMSO-HL60) were loaded with 0.25 (C) or 5 μM DCFH-DA (A,B) at 37 °C for 10 min and then stimulated at 37 °C for 15 min with (+) or without (–) 1.0 μM PMA. Cells were observed with a fluorescence microscope at 400× magnification and images were captured every 10 s as described in Materials and methods. During observation, the cells were continuously irradiated with excitation light. Cells were incubated with: (A) 5 μM DCFH-DA; (B) 5 μM DCFH-DA. After stimulation, VC was added to 50 mM and pH was adjusted to 5.0. Then the cells were incubated at 0 °C for 150 min. (C) Cells were incubated with 0.25 μM DCFH-DA. Although no fluorescent cells were visible in the four images (–), we confirmed that cells were present (–, bottom) with light microscopy.

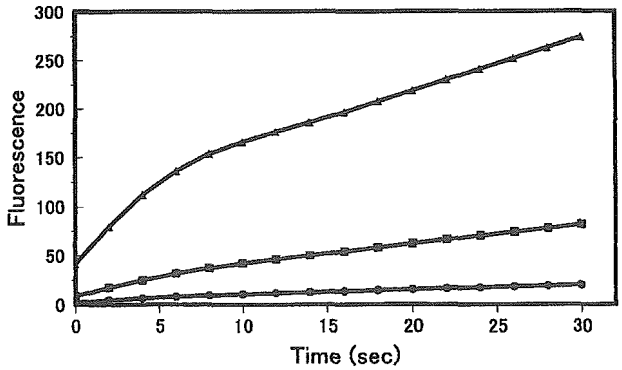

Fig. 9. Photoreaction of DCFH as dependent on DCFH concentration. The fluorescence increase in DCFH sample at 0.25 (●) 1.0 (■), or 5.0 μM (▲) during continuous irradiation at 500 nm with a 150 W xenon lamp was measured with wavelengths of 500 nm for excitation and 550 nm for emission. We selected an emission wavelength of 550 nm in this experiment because of the strong fluorescence of the 5.0 μM sample at 520 nm. Data were averaged from the results of four experiments.